TECHNICAL MEMORANDUM

293

Variational retrieval of temperature and humidity profiles from TRMM precipitation data

V. Marécal and J-F. Mahfouf

Research Department

November 1999

European Centre for Medium-Range Weather Forecasts
Europäisches Zentrum für mittelfristige Wettervorhersage
Centre européen pour les prévisions météorologiques à moyen

Abstract

This paper examines the performance of a one-dimensional variational (1D-Var) assimilation of TRMM derived surface rainfall rates from the Microwave Imager TMI. Temperature and specific humidity profiles are retrieved that are consistent with both observed and model short-range forecast rainrates. The assimilation uses the adjoint of moist physical parametrizations (deep cumulus convection, large-scale precipitation) to solve the minimization problem. Two atmospheric situations are examined from ECMWF short-range forecasts at $T_L319L31$ resolution. They encompass tropical cyclones, frontal bands and mesoscale convective systems. Results show that 1D-Var is generally able to find modified profiles within the range of forecast errors (specified from the operational ECMWF statistics) that provide a precipitation field close to observations. Because the convective and large-scale precipitation schemes do not produce very high surface rainrates, 1D-Var analysed profiles match less accurately observations in heavy precipitation areas. Increments of temperature with respect to the background state are small indicating that 1D-Var essentially adjusts specific humidity to modify precipitation amounts. Consistency checks have been defined in order to discard profiles producing too large departures from the observed rainfall rates or having too little sensitivity of model rainrates to changes in temperature and humidity. Moreover, the current 1D-Var approach is unable to modify profiles when the model rainrate is zero and the observed rainrate is non-zero. Sensitivity experiments are performed to the specification of observation errors. Observation errors are increased from 25 % of the observed value to 50 %. It is shown that 1D-Var is still able to assimilate some information from observations. However, an arbitrary threshold observation error needs to be set for light or no surface rainrates in the 1D-Var to avoid unrealistic increments of temperature and humidity. To decrease the computational cost of 1D-Var, two simplifications are explored: a reduction of the control vector by not including temperature profiles and the use of one background field and one observation field instead of seven for each assimilation window. These two approaches will be further evaluated when 1D-Var products are assimilated in the ECMWF four-dimensional variational system (4D-Var).

1 Introduction

The latent heat released by tropical rainfall plays a crucial role in driving the low-latitude atmospheric circulation and affects the weather around the world. However, conventional rainfall measurements are scarce in the tropics. Satellite observation is thus the only effective way to provide continuous monitoring of precipitation events. The Tropical Rainfall Measuring Mission (TRMM), which was launched in November 1997, aims at measuring rainfall and energy (i.e. latent heat of condensation) exchanges of tropical and subtropical regions (between 39°S and 39°N). This is the first Earth observation satellite to have on board a precipitation radar (PR), in association with microwave (TMI) and visible/infra-red (VIRS) imaging radiometers (Simpson et al., 1996; Kummerow et al., 1998).

Accurate measurements of satellite-derived rainfall rates provided by TRMM could be used in Numerical Weather Prediction (NWP) for improving the quality of operational analyses and forecasts. Indeed, most NWP models have difficulties in producing realistic weather elements, such as clouds and precipitation, at the beginning of the forecast period. This "spin-up problem" corresponds to an imbalance of the hydrological cycle during the first hours of the forecast and is generally more pronounced in the tropics than in the mid-latitudes. Currently, no operational global NWP model assimilates tropical rainfall observations on a routine basis. Various feasibility studies have been performed with global NWP models at ECMWF (Heckley et al., 1990; Puri and Miller, 1990), at FSU (Krishnamurti et al., 1984; Krishnamurti et al., 1993; Tsuyuki, 1996ab; Tsuyuki 1997) and at NCEP (Treadon 1996, Treadon 1997). The first approaches used in global models were based on diabatic normal mode initialization and on "physical initialization". Even though there is evidence that diabatic normal mode balance based on Machenhauer's scheme is not appropriate at low latitudes (Errico and Rash, 1988), substantial impact on the analyses (improved divergence field) were found by Heckley et al. (1990) and Puri and Miller (1990) using satellite rainrates derived from outward-going longwave radiation. Results from "physical initialization" (nudging of rain rate or rain-related quantities) studies also showed an improvement of the moisture analysis and a reduction of the spin-up problem. More recent approaches, such as three-dimensional (3D-Var) or four-dimensional (4D-Var) variational assimilations, can explicitly take into account model and observation errors and provide an optimal initial state. Treadon (1997) has assimilated in the NCEP 3D-Var system satellite derived rainfall rates from GOES Precipitation Index and from SSM/I (Special Sensor Microwave/Imager) brightness temperatures. First results showed a reduction of the precipitation spin-down and improved forecasts of the divergent wind at 200 hPa within the tropical belt. In parallel, Tsuyuki (1996ab, 1997) showed the feasibility of a simplified 4D-Var assimilation of SSM/I derived precipitation rates using a low-resolution version of the FSU global spectral model. He found a slight improvement over the tropical oceans.

We propose in this paper a two-step approach to assimilate observed precipitation in a global NWP analysis system. Firstly, a one-dimensional variational (1D-Var) assimilation of satellite derived rainrate observations is applied. It enables the retrieval of modified temperature and humidity profiles that provides precipitation rates consistent with both observations and

a model short-term forecast. Secondly, 1D-Var analysed products are introduced in a data assimilation system. The second step can be achieved more easily compared to a direct assimilation of precipitation rates since temperature and humidity variables are already operationally assimilated in 3D-Var or 4D-Var systems.

The 1D-Var assimilation of precipitation has already been studied in a theoretical framework (i.e. using simulated observations) by Fillion and Errico (1997) and Fillion and Mahfouf (1999). Fillion and Errico (1997) have shown that a 1D-Var method is able to make a significant adjustment of model precipitation rate within the range of realistic background temperature and specific humidity errors and rainrate observation error. Their study was restricted to convective regimes, and large-scale precipitation processes were disregarded. Fillion and Mahfouf (1999) (denoted FM99 hereafter) focused their study on the coupling of moist-convective and stratiform precipitation processes in 1D-Var. Three convective parameterizations were tested by FM99. They showed that the vertical structure of increments produced by the 1D-Var strongly depends upon convective parametrization. They also demonstrated that the introduction of stratiform precipitation can control the minimization at the expense of convective precipitation for slightly supersatured profiles.

Treadon (1997) also used a 1D-Var framework to test a 3D-Var assimilation of satellite derived rainrates. He showed that 1D-Var performed well on real data although it is more successful for decreasing rather than increasing precipitation to get closer to observations.

In the present work we use the version of 1D-Var developed by FM99 based on the ECMWF mass-flux convective scheme. This study focuses on the behaviour of 1D-Var in the context of real data assimilation. TMI (TRMM Microwave Imager) derived surface rainrates have been selected for assimilation because of their good accuracy. This work on 1D-Var assimilation should be regarded as a first step. The second step, regarding the assimilation of 1D-Var products in the ECMWF 4D-Var system (Rabier et al., 1999), will be the subject of a forthcoming paper.

Section 2 presents the 1D-Var method with special emphasis on modifications to the original FM99's 1D-Var. The TRMM data set to be assimilated in 1D-Var is described in section 3. Results of a control experiment are discussed in section 4. Section 5 is devoted to results of various sensitivity tests. Finally, the conclusions are given in section 6.

2 The 1D-Var method

2.1 Basis

Let $\mathbf{x}$ be the vector which represents the atmospheric state (called hereafter control variable) and R_o the collocated surface rainfall rate estimated from TRMM data. The 1D-Var retrieval consists of finding an optimum state $\mathbf{x}^a$ which minimizes a distance between the model rainfall rate and R_o, given a background constraint provided by the error covariances of a short term forecast profile $\mathbf{x}^b$. If the background and observation errors are uncorrelated and each has a Gaussian distribution, the maximum likelihood estimator of the state vector $\mathbf{x}$ is the minimum of the following cost-function:

$$J(\mathbf{x}) = \frac{1}{2}(\mathbf{x}-\mathbf{x}^b)^T\mathbf{B}^{-1}(\mathbf{x}-\mathbf{x}^b) + \frac{1}{2}\left[\frac{R(\mathbf{x})-R_o}{\sigma_o}\right]^2 \quad (1)$$

where $\mathbf{B}$ is the background error covariance matrix, σ_o the standard deviation of observation error (in theory, errors from the observation operator should also be included). $R(\mathbf{x})$ is a calculation of surface rainrate from the atmospheric state $\mathbf{x}$ at the observation location. As in FM99, the control variable vector contains 63 elements: profiles of temperature T and specific humidity q on 31 model levels and surface pressure P_s.

The minimization module is a limited memory quasi-newton (M1QN3) which requires an estimation of the gradient of the cost function at each iteration (Gilbert and Lemaréchal, 1989). A preconditioning procedure similar to Fillion and Errico (1997) is applied for improving the convergence. The gradient of $J(x)$ is given by:

$$\nabla J(\mathbf{x}) = \mathbf{B}^{-1}(\mathbf{x}-\mathbf{x}^b) + \mathbf{R}^T\left[\frac{R(\mathbf{x})-R_o}{{\sigma_o}^2}\right] \quad (2)$$

The operator $\mathbf{R}^T$ is the transpose of the Jacobian matrix of the partial derivatives of rainfall rates with respect to the input profile (i.e. adjoint of the tangent-linear of the moist physical processes). Given the low dimension of the control vector (63 variables here), the Jacobian elements are computed explicitly in finite differences by a perturbation method requiring 64 calls (63 perturbations and one reference) to the non-linear observation operator $R(\mathbf{x})$.

2.2 Observation operator

The observation operator $R(\mathbf{x})$ includes two components which are the moist-convective (noted CO hereafter) parameterization and the non-convective precipitation or stratiform precipitation (noted ST hereafter) parameterization.

A diagnostic parameterization of stratiform precipitation based on a moist-local adjustment process is used as in FM99. In this scheme, the excess of moisture with respect to saturation at a given level is converted into non-convective precipitation. The adjusted values of temperature and specific humidity correspond to a saturation state and are obtained by keeping the moist static energy constant. Evaporation of precipitation in sub-saturated layers is accounted for.

The convective parameterization is the ECMWF operational mass-flux scheme originally developed by Tiedtke (1989). The statistical cloud population is described through a single bulk entraining plume model. For deep convection, the Tiedtke's original moisture convergence closure is replaced by a closure based on the reduction of CAPE towards zero over a given time scale τ depending on model truncation (Gregory et al., 1999). Here τ is 1400s to be consistent with the ECMWF operational model. In the present study the convective scheme is not coupled to the operational prognostic cloud scheme (Tiedtke, 1993). Therefore, all detrained liquid water from convective clouds is assumed to evaporate instantaneously in the environment.

The coupling of moist-convection and stratiform precipitation schemes follows the Fractional-Stepping (FS) approach (Beljaars, 1991). This means that the convective precipitation operator is applied first. Then, the stratiform precipitation parameterization acts on an atmospheric state already affected by the convective precipitation operator. The alternative approach is called Process Splitting (PS) (Beljaars, 1991) where convection and stratiform precipitation operators are applied to the same atmospheric state. The FS approach is chosen to be consistent with the ECMWF coupling of physical parameterizations. Moreover, FM99 showed that using FS instead of PS strongly reduces the frequency of unrealistic supersaturations in the humidity profiles retrieved by the 1D-Var method. These supersaturations correspond to cases where the minimization mostly modifies stratiform precipitation at the expense of convective precipitation. Nevertheless, in few cases the FS approach is also not able to control large supersaturations. This point will be discussed again in section 4.

To perform the 1D-Var analysis, background profiles have to be collocated with the observations. This can be achieved by an horizontal interpolation of the background fields at the observation location. But applying an horizontal interpolation induces modifications of humidity and temperature profiles. FM99 have studied the sensitivity of the CO parameterization to variations of specific humidity and temperature. Their Figure 3 shows that surface rainrate is highly sensitive to humidity variations at the lowest model level. Preliminary tests have proved, that for some profiles, horizontal interpolation can lead to unrealistic changes in the amount of precipitation produced by the convection scheme when compared to the non-interpolated background precipitation. To avoid horizontal interpolation of model fields and reduce representativeness problems, rainfall observations have been averaged within model grid boxes.

2.3 Background profiles

Since quantities retrieved using 1D-Var will be assimilated in the ECMWF operational 4D-Var analysis system, the 4D-Var configuration is used to define background fields. The current operational 4D-Var assimilation window of six hours is divided in seven time slots in order to compare observations at the appropriate time. In this study, two atmospheric situations are examined. Temperature and specific humidity profiles and surface pressure were produced from two short-range forecasts starting on 10 February 1998 at 1800 UTC and on 26 August 1998 at 0600 UTC from the ECMWF model with spectral truncation T_L319 (corresponding to a 60 km resolution approximately) and 31 vertical levels.

In FM99, only the control variables (profiles of T and q and P_s) were used in the observation operator to calculate surface rainrate. In the forecast model at each time step, tendencies from the dynamics and other physical processes modify the input profiles of the moist parameterizations. In the present study, we chose to include, as input to the 1D-Var, profiles of temperature and specific humidity tendencies after dynamical processes, radiation, turbulence and gravity wave drag parameterizations are applied. Even though these tendencies are kept constant during the minimization they enable the precipitation field from the 1D-Var background state to be more consistent with the three-dimensional environment of the short-range model forecast.

2.4 Background error statistics

As in FM99, the covariance matrix of background errors $\mathbf{B}$ is taken from the operational ECMWF 4D-Var system (Rabier et al., 1997; Derber and Bouttier, 1999). The covariance coefficients are computed statistically using the NMC method (Parrish and Derber, 1992) from differences between 48-hour and 24-hour forecasts. As in the ECMWF 4D-Var analysis system, no cross-correlations between background errors of specific humidity and temperature are considered. An example of vertical profiles for standard deviation of temperature and specific humidity is given in FM99 (see their Figure 2). Observations from TRMM being restricted to the tropics, background errors of "unbalanced" temperature are chosen (Derber and Bouttier, 1999). Thus, standard deviations over the vertical are less than 1 K. The vertical distribution of standard deviation for specific humidity exhibits a maximum at level 25 (around 850 hPa), an exponential decrease above and lower values in the boundary layer. This profile has been empirically specified by Rabier et al. (1997).

3 Observations

The observations from the TRMM mission selected for this study are the instantaneous surface rainfall rates estimated from TMI radiometer that are provided operationally (product 2A12

level 4) by NASA. They are calculated from the profiling algorithm developed by Kummerow et al. (1996) using a cloud data base coupled to a microwave radiative transfer model.

To be consistent with the analysis dates/times chosen, the data sets selected correspond to TMI observations from 10 Feb. 1998 at 2100 UTC to 11 Feb. 1998 at 0300 UTC and from 26 Aug. 1998 at 0900 UTC to 26 Aug. 1998 at 1500 UTC. As in the operational 4D-Var assimilation system, the six hour observations are divided in seven time slots. The first and the last slots are half an hour long and the other five slots are one hour long.

In the following, the February case is chosen to illustrate most of the 1D-Var results. For this case, a large variety of oceanic precipitation has been observed during the six hour window: an intense tropical cyclone in the Indian Ocean, four frontal systems and mesoscale convective systems over the East Tropical Pacific and over the East Indian Ocean. For the August case, a hurricane (Bonnie), two fronts and several tropical convective systems were sampled by TMI. Note that fronts are usually not observed in their full extent because of the limited TMI latitude coverage (between -39° to +39° latitude).

TMI 2A12 instantaneous surface rainrates are provided for each high resolution pixel corresponding to an area of about 7×5 km^2. The swath width of 758.5 km is covered by 208 high resolution pixels. Since TMI-2A12 rain estimations over land are less reliable than over ocean (Kummerow et al., 1996), only observations over sea have been considered in this study. The TMI surface rainrates used in 1D-Var were obtained by averaging high resolution rainrates over the model gridboxes. This is done to be consistent with the surface precipitation calculated by the model which represents the mean of precipitation and/or no-precipitation areas in the model grid box. Moreover, since the model is not able to represent small scale precipitation, each mean surface rainrate corresponding to a precipitation coverage of less than 10 % in a grid box is set to zero. In practice, this procedure filters out most mean rainrates smaller than 0.1 mm h^{-1}. The mean resulting observation field is shown in Figure 1 for the February case. This situation will be analysed in details in the following and the August case will be used to evaluate the generality of our results. For this figure and the followings, three representative limited areas are chosen to illustrate the results obtained in this study. They correspond to the major types of meso and large scale precipitation systems encountered between -40 and +40 degrees latitude: a tropical cyclone sampled on 11 Feb. 1998 around 0140 UTC (Fig. 1a), mesoscale convective areas sampled on 11 Feb. 1998 around 0240 UTC (Fig. 1b) and a front sampled on 10 Feb. 1998 around 2305 UTC (Fig. 1c).

To solve Equation (1), it is necessary to set the observation error σ_o. Precipitation rate is a positive quantity and therefore its associated errors are not normally distributed. Errico et al. (1999) showed, in a theoretical context, that using non-normal distributions have a significant impact on 1D-Var analysed state. But because no estimation of TMI 2A12 surface rainrate error and its associated distribution is yet available, a Gaussian distribution of errors was assumed for simplicity. A reasonable value of root mean square of 25 % of R_o was chosen. Since Equation (1) is not defined if the observation is perfect (zero observation error), a threshold value of 0.01 mm h^{-1} was chosen for the smallest possible observations error. Since these choices are somewhat

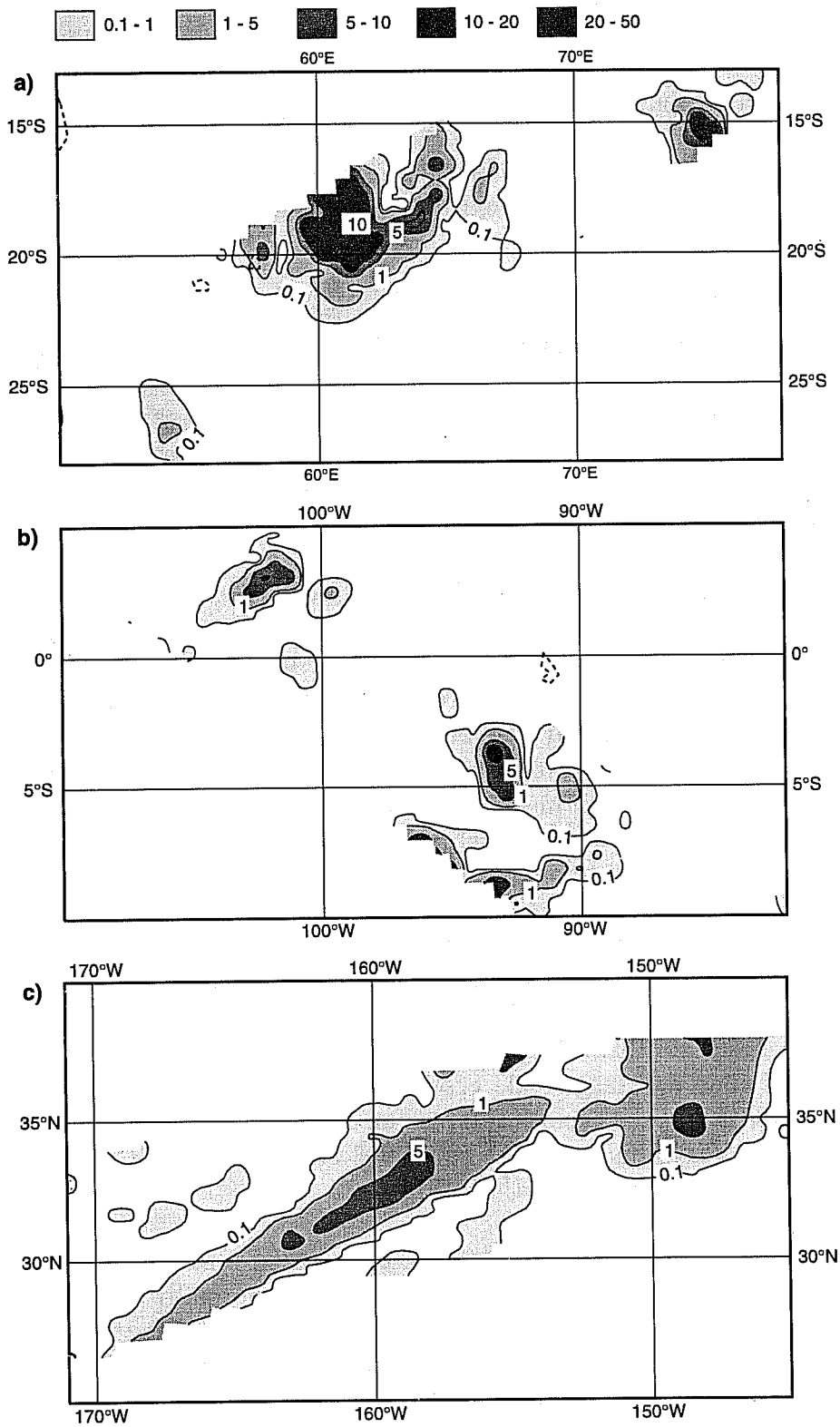

Figure 1: *Instantaneous mean observed TMI surface rainrate in mm h^{-1} (R_o field) in (a) South Indian Ocean, (b) Central Pacific Ocean and (c) North Pacific Ocean along TRMM track between 10 Feb. 1998 at 2100UTC and 11 Feb. 1998 at 0300 UTC.*

arbitrary, sensitivity of the results to the specification of observation errors was tested. This aspect is discussed in section 5.

4 Results

Results discussed in this section will be considered in the following as Control experiment.

4.1 1D-Var background precipitation

The surface rainrate field obtained applying the observation operator to the background profiles (called background rainrate and noted R_b hereafter) is displayed in Figure 2. This field is obtained from a one time-step integration of the moist physical processes in stand-alone mode. It is important to verify that this 1D-Var background rainrate field compares reasonably well with the instantaneous rainrate produced from the forecast model, and referred herafter as 4D-Var background rainrate field. This 4D-Var background rainrate field is presented in Figure 3. Comparison between the two background rainrate fields shows that, for precipitation generated by convection, location and intensity are similar as illustrated by Figs. 2ab and 3ab. Frontal precipitation has similar intensity but is much less extended in the R_b field (Figs. 2c and 3c). The main reason for this difference is the use of a diagnostic ST scheme. This scheme is less efficient at triggering stratiform precipitation than the operational prognostic ST scheme which uses additional dynamical information from the forecast model (Tiedtke, 1993; Gregory et al., 1999). Nevertheless overall, 1D-Var and 4D-Var background surface rainrates fields are in good agreement.

Comparison between R_b (Fig. 2) and R_o fields (Fig. 1) exhibits the following general differences:

- tropical cyclones are weaker and more diffuse in R_b (see Figs. 1a and 2a). Location is generally similar although it is sometimes shifted by few grid points when the short range model forecast (4D-Var background) is not accurate enough.

- mesoscale convection is often forecasted and observed in the same area but not localized exactly at the same place in R_b and R_o as shown in Figures 1b and 2b.

- frontal systems are less extended in R_b than in R_o field (see Figs. 1c and 2c). Precipitation location in field R_b can also be slightly shifted with respect to R_o field like for tropical cyclones. This is the case for the frontal zone chosen here to illustrate results (see Figs. 1c and 2c).

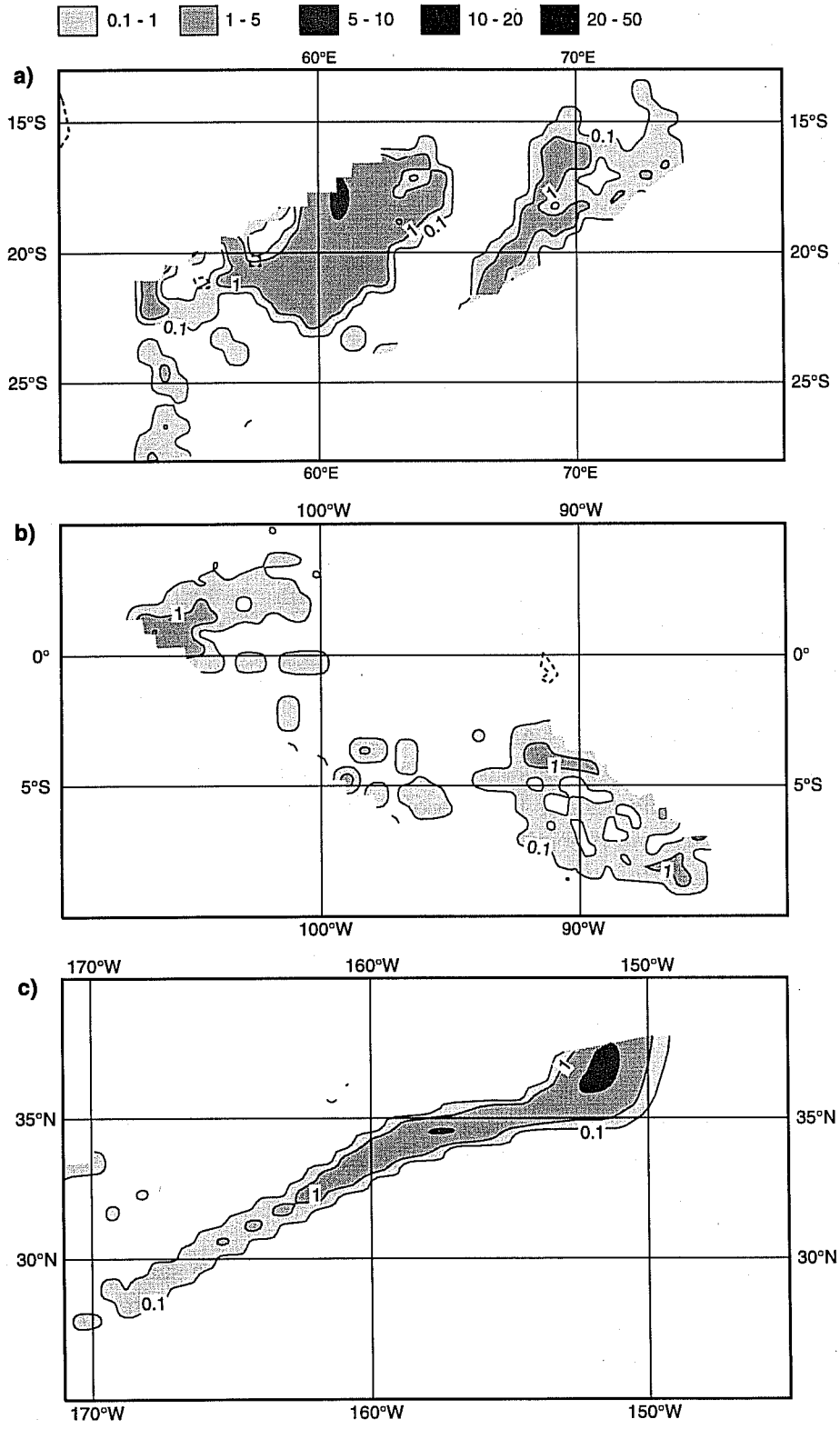

Figure 2: *Same as Figure 1 but for 1D-Var background surface rainrate (R_b field).*

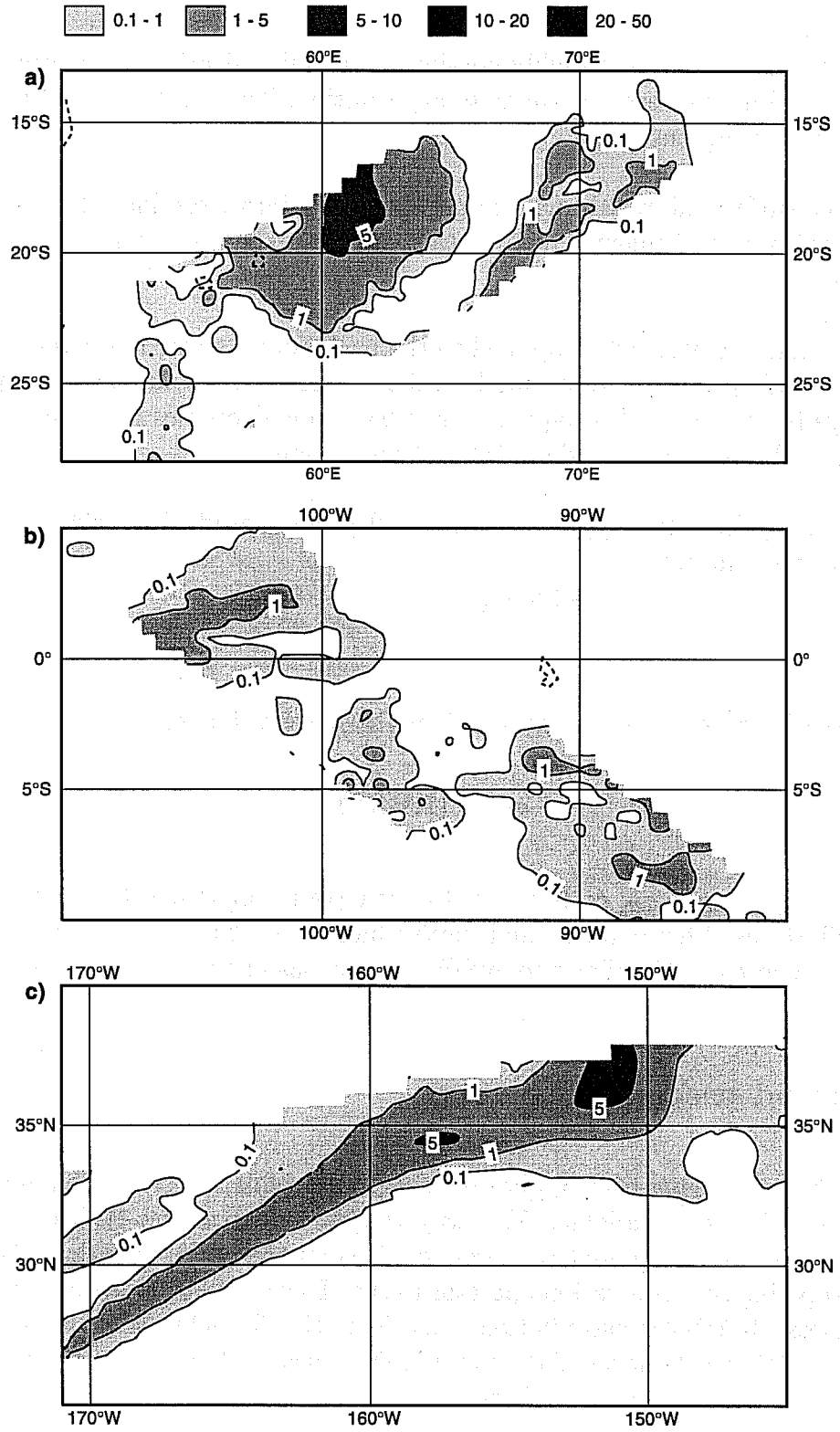

Figure 3: *Same as Figure 1 but for 4D-Var background surface rainrate.*

4.2 Analysis criteria

Since the observation operator is highly non-linear, the minimization procedure cannot always reach a realistic solution or even converge to any solution. These extreme and infrequent cases correspond to two situations:

1- TMI observed surface rainrate is much larger than the rainrate produced from the background state (by several orders of magnitude). In this case, the 1D-Var minimization is not able to find a solution.

2- The observation operator, when applied to the background state, has a very low sensitivity to temperature and specific humidity modifications leading the minimization to produce unrealistically large increments. This happens when background profiles produce very low surface rainrates and TMI observations indicate almost no rainfall.

To avoid analysing these two types of profiles, all profiles producing background departures outside the following limits:

$$-100\sigma_{R_b} < R_b - R_o < 5\sigma_{R_b} \tag{3}$$

are discarded.

Here σ_{R_b} is the background error expressed in the observation space (i.e. surface rainrate) using:

$$\sigma_{R_b} = \left(\mathbf{R}\mathbf{B}\mathbf{R}^T\right)^{1/2} \tag{4}$$

A low (resp. high) value of σ_{R_b} corresponds to a low (resp. high) sensitivity of the background state to modifications of temperature and specific humidity. Thus, the negative (resp. positive) boundary value chosen in (3) allows to avoiding situations of type 1 (resp. type 2).

4.3 Analysed precipitation

Once the 1D-Var method has been applied to background fields, analysed profiles of temperature and specific humidity are available. To verify the behaviour of the 1D-Var assimilation the analysed precipitation field (noted R_a hereafter) is compared to observations. The R_a field is obtained by applying the observation operator to the 1D-Var analysed temperature and specific humidity profiles. If 1D-Var assimilation is efficient, the R_a field should be close to TRMM surface rainrate field to the level of the prescribed accuracy of the observations. The R_a field for the February case is displayed in Figure 4.

For the interpretation of the results, two types of profiles are discussed separately. Firstly, when 1D-Var background precipitation is greater than zero ($R_b > 0$), the 1D-Var analysis is

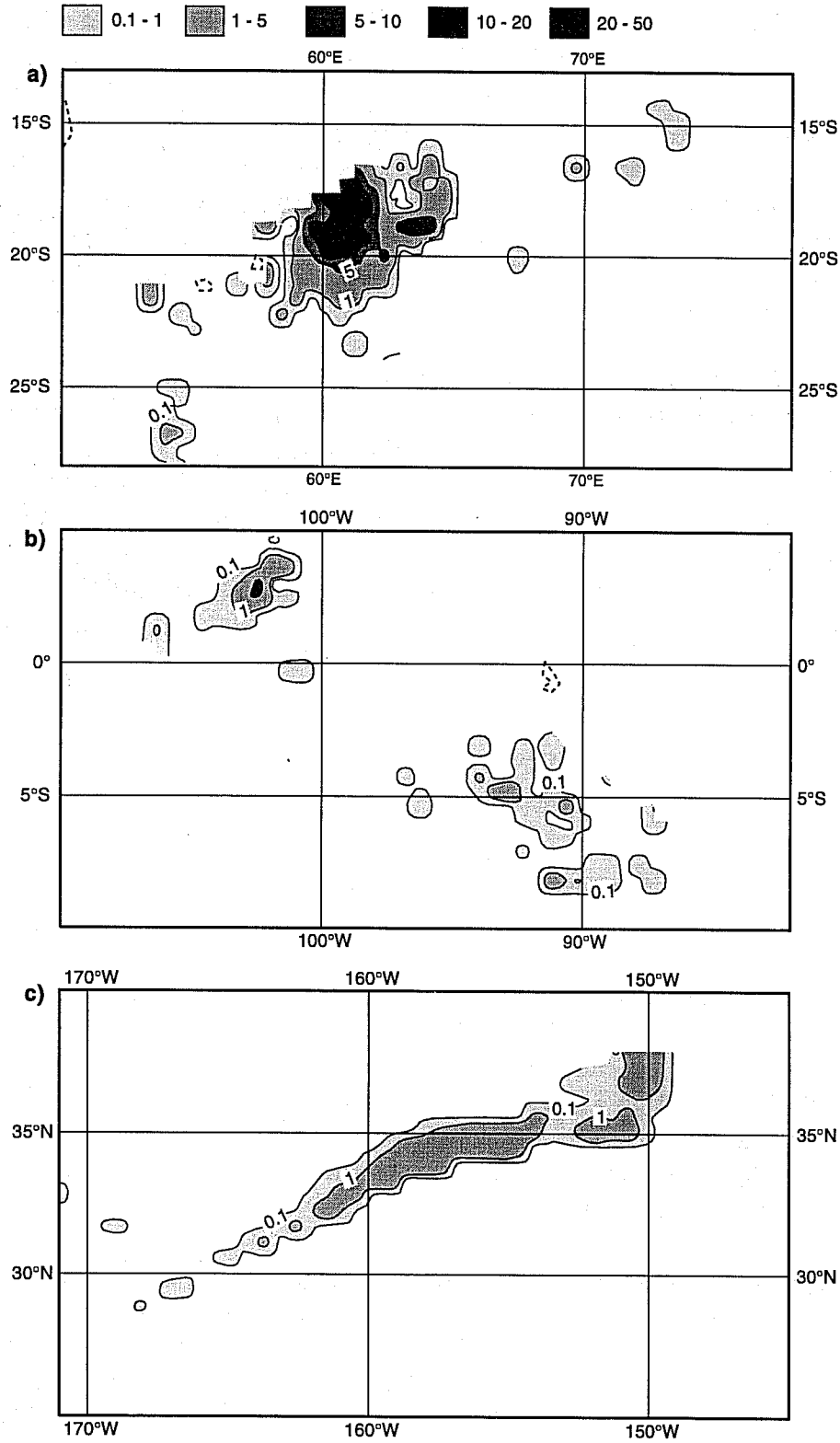

Figure 4: *Same as Figure 1 but for 1D-Var analysed surface rainrate (R_a field) for control experiment. Background surface rainrate is used for profiles not satisfying the criteria of formula (3).*

generally able to increase, decrease and even switch-off precipitation as required, except for cases of heavy precipitation where analysed rainrates never reach observed values. This result is well illustrated for the tropical cyclone (Fig. 4a) where the precipitation structure in the R_a field is similar to observations. Surface rainrate is increased by about 7 mm h^{-1} in the central part of the cyclone but still remains weaker than R_o. Part of the difference can be explained by the large observation error associated to intense observed rainrates which leads to reduced weight for the observation term in the cost function with respect to the background term. These results agree with Treadon (1997) who found, using a constant observation error of 0.5 mm h^{-1}, that his 1D-Var was better at handling a decrease of precipitation with respect to background than an increase.

The second type of profiles to be discussed corresponds to $R_b = 0$. In this case, σ_{R_b} is zero because there is no sensitivity of the background state to small increments of temperature and specific humidity. In other terms, 1D-Var assimilation is not able to trigger precipitation by modifying temperature and humidity profiles. Consequently, profiles with $R_b = 0$ cannot be analysed by 1D-Var when precipitation exists in the observation field (see for instance Figs. 1b, 2b and 4b). In the frontal zone displayed in Fig 4c, this leads to a global decrease of precipitation as a consequence of a phase shift in the precipitation patterns between R_b (Fig. 2c) and R_o (Fig. 1c) fields. Treadon (1997) found the same behaviour of his 1D-Var for non-rainy background profiles.

4.4 Statistics

A more general view of the 1D-Var behaviour for the whole 6-hour data set is given in Table 1. For the February case, the number of profiles "missed" by 1D-Var ($R_o \neq 0$ and $R_b = 0$) is comparable to the total number of profiles analysed by 1D-Var and mostly corresponds to frontal and mesoscale convective precipitation. This number is usually smaller for other cases, as illustrated by the August case, the number of fronts generally sampled in six hours being smaller (one or two). For both case studies, the number of points which do not satisfy the 1D-Var analysis criteria (Equation 3) is small compared to the total number of 1D-Var analysed points. It was verified that all rejected profiles correspond to cases where 1D-Var analysis would provide unrealistically large increments in absolute value or no increments at all, leading to no modification of R_b while expected to get closer to R_o.

Figure 5 displays the histograms of $(R_b - R_o)$ and $(R_a - R_o)$. The corresponding bias and standard deviation are given in Table 2 (see page 21). This figure clearly shows that the 1D-Var assimilation has been able to provide an analysed state closer to observations with a reduction of the standard deviation from 2.01 mm h^{-1} to 0.80 mm h^{-1}. The histogram for $(R_b - R_o)$ extends further in negative values (minimum = -17.3 mm h^{-1}) than in positive values (maximum = 7.1 mm h^{-1}). This is related to the model behaviour which always produces precipitation areas which are more extensive and less intense than observed for very active convective systems, as shown in Fig. 3 and Fig. 1. The 1D-Var analysis produces an important reduction of the

Experiment	Analysis date/time	Number of analysed) profiles (ST)	Number of $R_b \neq 0$ and $R_o > 0$ profiles	Number of rejected profiles by formula (3)
Control	11 Feb. 1998 00 UTC	2685 (383)	2680	80
Control	26 Aug. 1998 12 UTC	2667 (151)	2196	10
Test 4	11 Feb. 1998 00 UTC	2238 (227)	2330	63
Test 4	26 Aug. 1998 12 UTC	2260 (105)	1959	8

Table 1: *Results of 1D-Var analysis for 6-hour periods for control and test experiments. In parenthesis are given the number of profiles analysed where ST parameterization is active.*

histogram range with minimum and maximum values for $(R_a - R_o)$ of -12.9 mm h^{-1} and 2.5 mm h^{-1}, respectively. Very similar results are found for the August case as illustrated by the bias and standard deviation of $(R_b - R_o)$ and $(R_a - R_o)$ given in Table 2 which are close to those found for the February case.

Nevertheless, some profiles remain nearly unchanged by 1D-Var analysis leading to R_a values close to R_b and therefore far from the observation. This behaviour is illustrated in the scatter plot of Figure 6a where two families of points clearly appear. The first family corresponds to profiles close to the unit slope line where the 1D-Var analysis has modified the background state so that it provides a surface rainrate close to observations. Note that the fit to the unit slope line deteriorates when $(R_o - R_b)$ increases because 1D-Var is less efficient in increasing precipitation and to the fact that we specify larger observation errors for high rainrates. The second family of points in Figure 6a corresponds to $(R_a - R_b)$ values close to zero where no rainrate information from the observations is assimilated by 1D-Var. For these profiles, the non-linear behaviour of the physical parameterizations is such that the 1D-Var has been unable to find a minimum for the cost-function. In the context of 4D-Var assimilation of 1D-Var products, this second type of profile should not be retained because they would provide an information about the model background instead of an information about the observations. Thus, a quality control of the 1D-Var products based on a criterion excluding this second type of profiles will be applied before 4D-Var assimilation. Figure 6b presents 1D-Var products after a quality control has been applied. By retaining only analysed points where $R_o - \sigma_o < R_a < R_o + \sigma_o$, all the profiles were $R_a \simeq R_b$ are clearly rejected, but a significant amount of profiles are kept (78 %).

In their study, FM99 have shown that for some profiles the minimization is controlled by ST parameterization creating unrealistic stratiform precipitation where convective precipitation is expected. Table 1 shows that ST parameterization is involved in the minimization for a few hundred profiles depending on the number of fronts overpassed by TRMM in six hours. Even though supersaturations can be created by the 1D-Var for increasing stratiform precipitation, their locations correspond to intense precipitating areas where convection is also active. It seems reasonable that in intense convective systems part of the precipitation has a stratiform origin (Houze, 1997). The pathology shown by FM99 has not been evidenced in the present

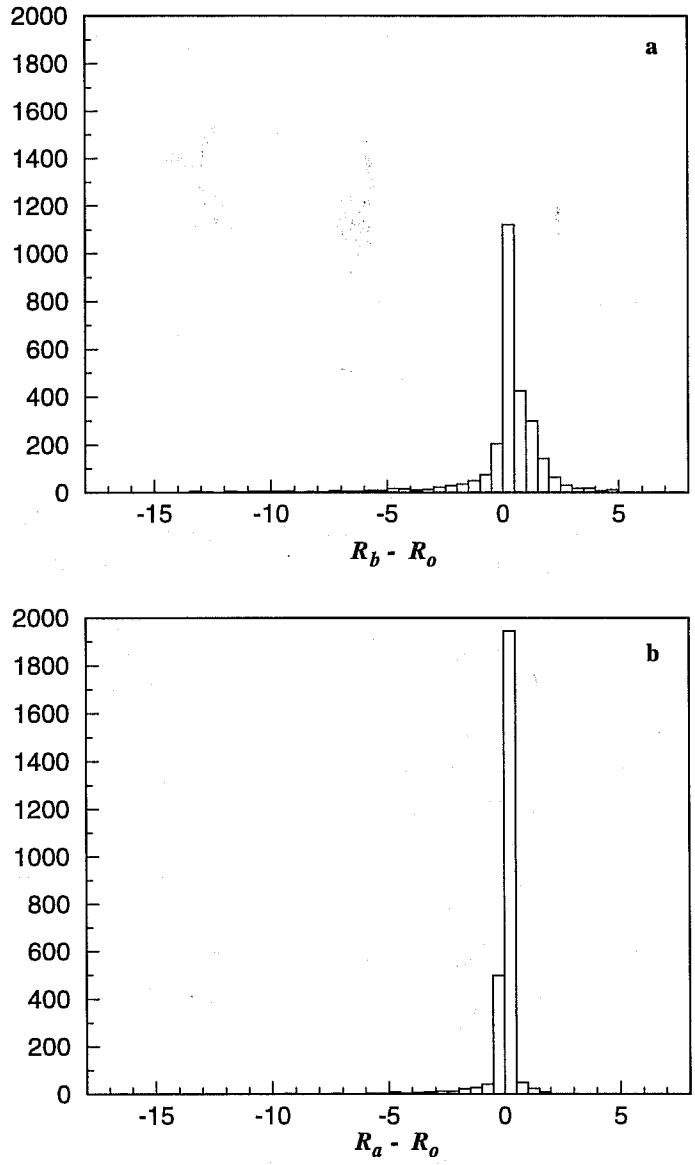

Figure 5: *Histogram of (a) $(R_b - R_o)$ in mm h^{-1} and (b) $(R_a - R_o)$ in mm h^{-1} for the Control experiment (11 Feb. 1998 0000 UTC).*

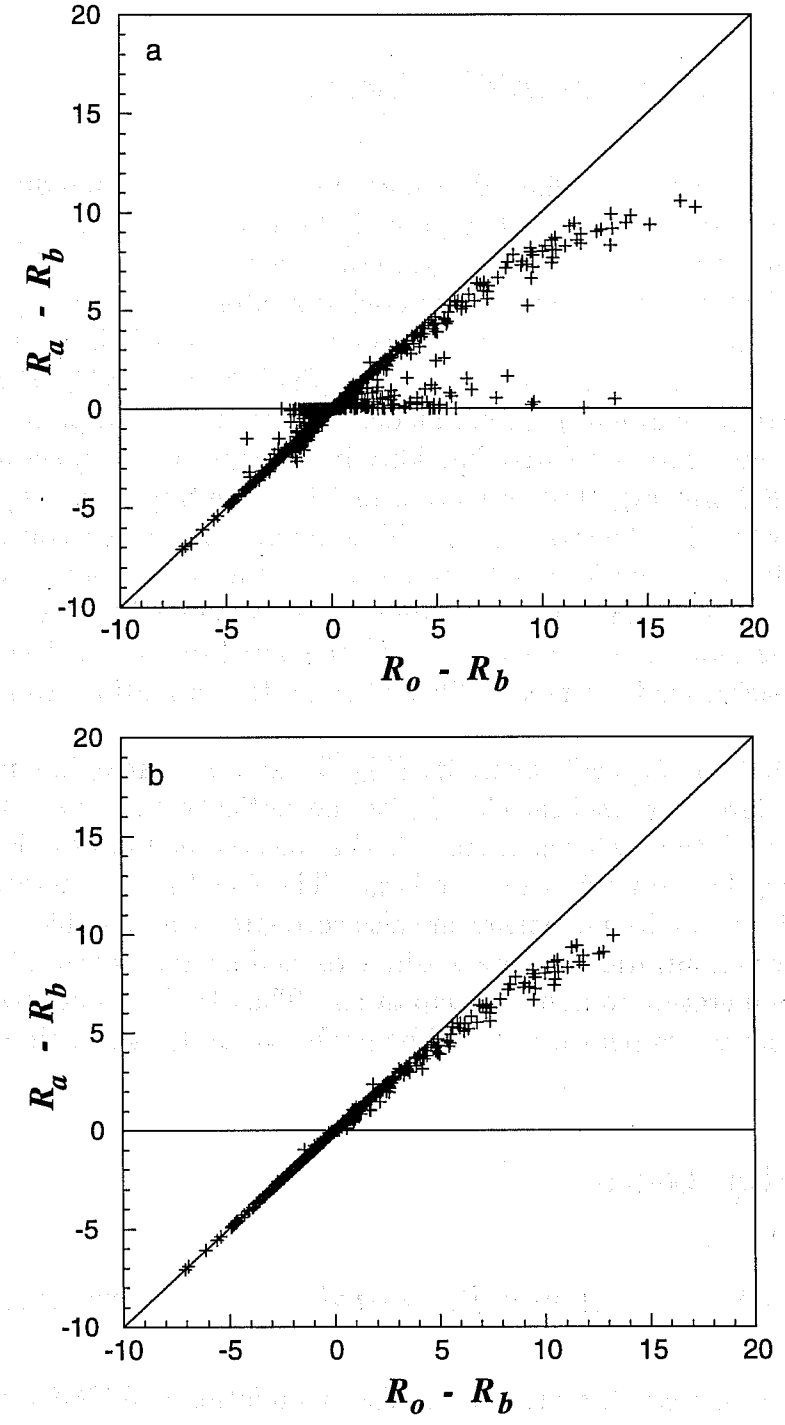

Figure 6: *Scatter plot of* $(R_a - R_b)$ *in mm* h^{-1} *as a function of* $(R_o - R_b)$ *in mm* h^{-1} *for the Control experiment (11 Feb. 1998 at 0000 UTC).*

results, which may suggest that this problem is marginal, at least with the ECMWF mass-flux convection scheme.

4.5 Temperature and humidity increments

The 1D-Var provides analysed profiles of temperature and specific humidity from which increments between the analysed and the background states ($\mathbf{x}_a - \mathbf{x}_b$) can be derived. They are represented in Figure 7 where the $R_o \geq R_b$ profiles (denoted MORE profiles) and the $R_o < R_b$ profiles (denoted LESS profiles) have been treated separately. For both types of profiles, mean temperature increments in absolute value are small with values below 0.10 K for all vertical levels (Fig. 7a). Mean specific humidity increments (Fig. 7b) reach 0.39 g/kg (resp. -0.13 g/kg) with a maximum (resp. minimum) around model level 24 for MORE profiles (resp. LESS profiles). The vertical structure of relative humidity increments (Fig. 7c) shows that, to increase precipitation (MORE profiles), 1D-Var analysis moistens the troposphere up to level 7 (around 130 hPa) and slightly dries the stratosphere. This behaviour is a consequence of the negative temperature correlations of background errors between the troposphere and the stratosphere. The contrary is found for LESS profiles. A similar result was found by Treadon (1997) but with more drying and less moistening. Differences may be related to the use of a different convection scheme, different background errors and different rainrate observation errors.

The vertical distribution of specific humidity (Fig 7b) and of relative humidity (Fig 7c) increments below model level 7 are well correlated with the vertical distribution of background errors for q (see Figure 2 in FM99). This is because 1D-Var mostly modifies specific humidity profiles where corresponding background errors are large. The fact that temperature increments are low and that relative humidity increments are also correlated with specific humidity increments means that 1D-Var minimization is more sensitive to modifications of specific humidity than to modifications of temperature to adjust precipitation. Thus 1D-Var products related to specific humidity rather than to temperature should be preferred for 4D-Var assimilation.

5 Sensitivity tests

5.1 Time tendencies of specific humidity and temperature

The main difference between the present 1D-Var assimilation and FM99 version is that time tendencies of temperature and specific humidity related to processes other than CO and ST (i.e. dynamics, radiation, gravity wave drag, vertical diffusion) have been used to update vertical profiles in the observation operator. To show the impact of this choice, R_b is recalculated by setting to zero these tendencies as in FM99. Results are displayed in Figure 8. Compared to the R_b control field (Fig. 2), convective precipitation is enhanced for heavy rates and

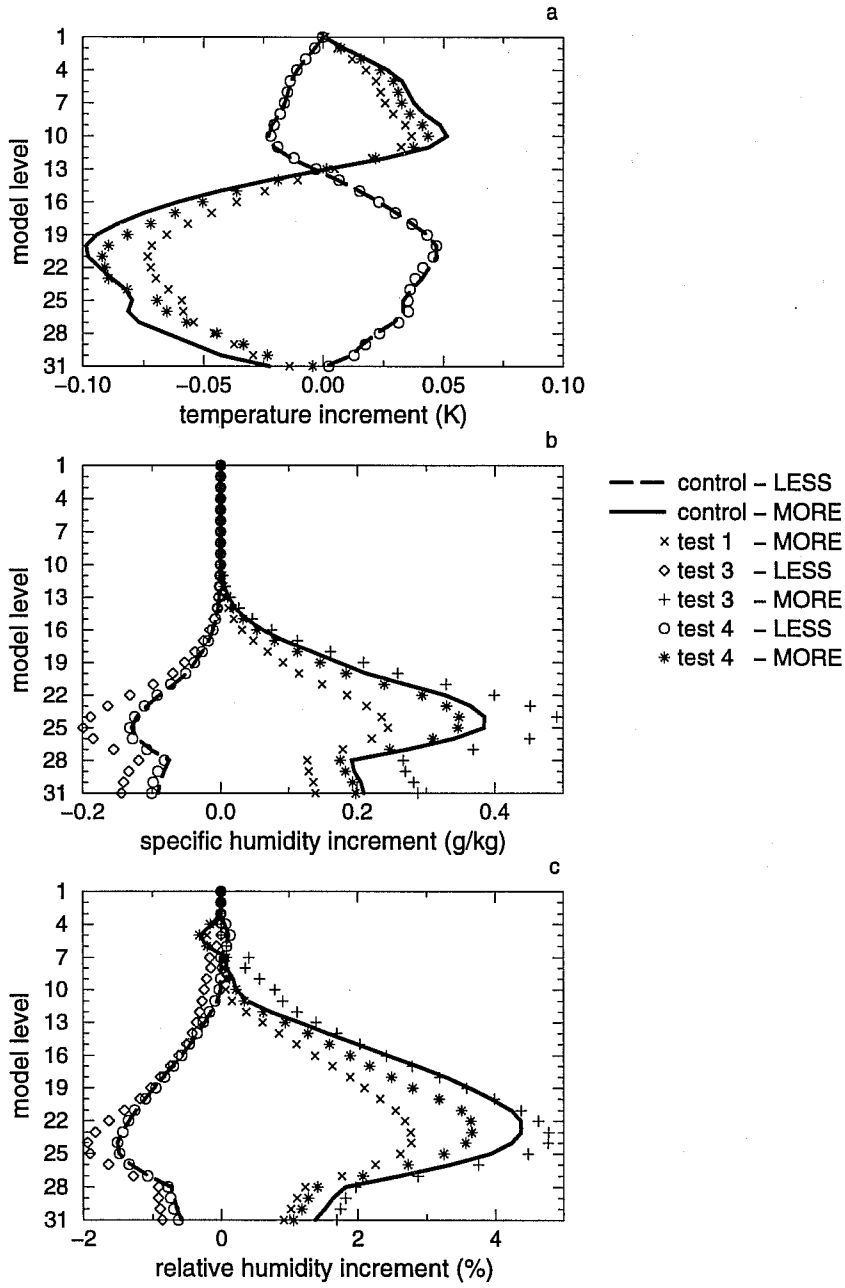

Figure 7: *Profiles of (a) mean temperature increments, (b) mean specific humidity increments and (c) relative humidity increments. The control and tests experiments are all from the February case. LESS and MORE are explained in the text.*

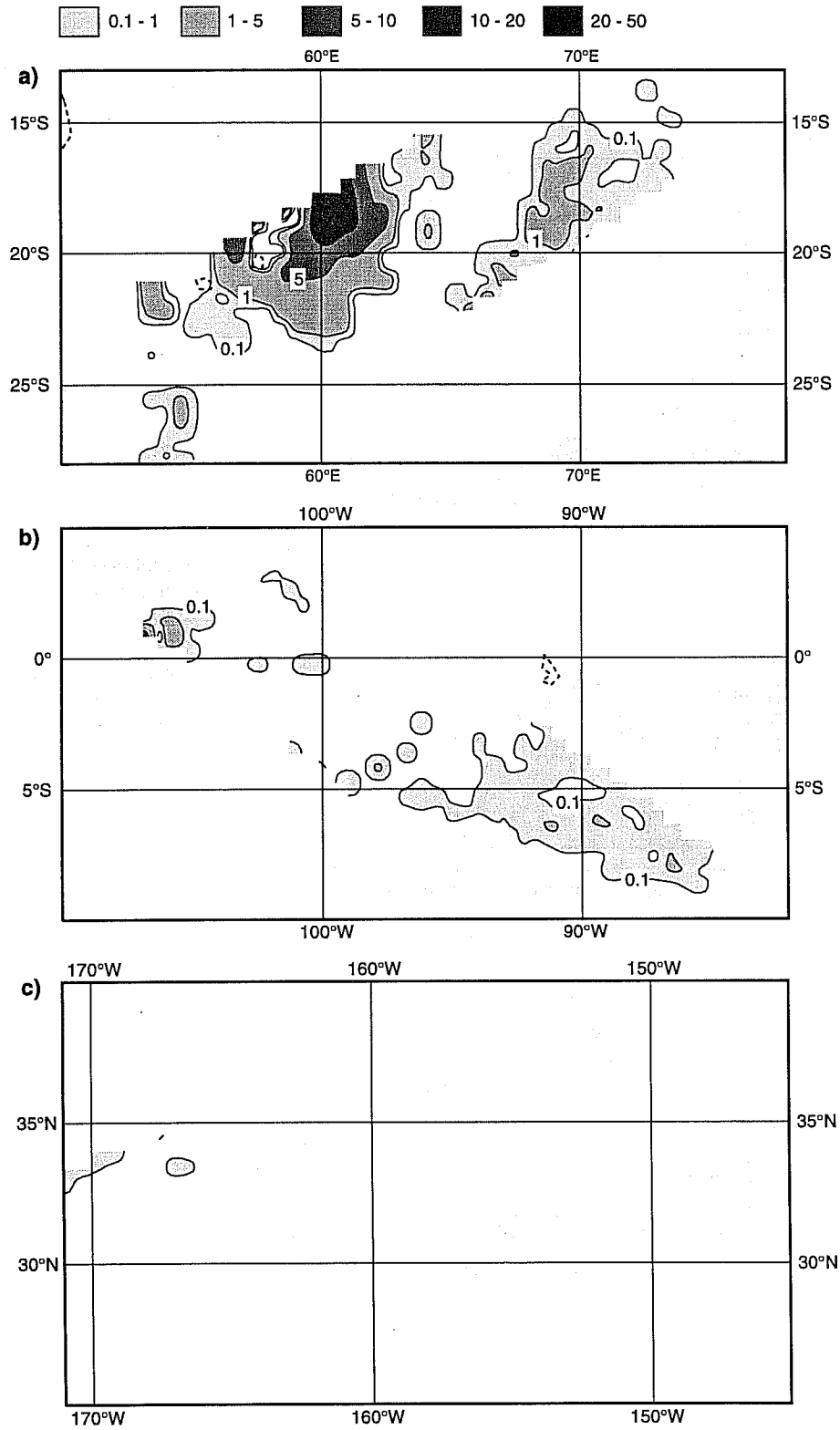

Figure 8: *Same as Figure 1 but for 1D-Var background surface rainrate calculated without using time tendency profiles of temperature and specific humidity.*

slightly reduced for light rates. Stratiform precipitation is largely reduced so that the frontal precipitation zone does not exist anymore (Fig. 8c). Comparison with the 4D-Var background rainrate field produced by the 3-D model (Fig. 3) shows even more differences. Thus, the R_b field calculated without thermodynamic time tendencies is clearly less consistent with the 4D-Var background rainrate field. This is because these time tendencies provide a major piece of information to CO and ST schemes concerning the environment in which precipitation is formed. They are essential to ensure that CO and ST parameterizations behave similarly in the one-dimensional and three-dimensional contexts.

5.2 Observation error

As discussed in section 3, the observation error used in Eq. (1) is based on rough estimation. A first sensitivity test (experiment noted Test 1) has been run with an observation error set to $0.50 \times R_o$ instead of $0.25 \times R_o$ and no modification of the threshold error for low observed surface rainrates. This increase of the observation error can also be interpreted as an indirect way to take into account errors coming from the observation operator. Test 1 experiment produces an increase of the negative bias and a larger standard deviation of the analysis departure $(R_a - R_o)$ compared to the control (see Table 2). For moderate and heavy observed rainrates, the observation term in the cost function is smaller for Test 1 experiment leading to a weaker constraint from observations in the minimization. This effect also appears on the MORE profiles of specific humidity, temperature and relative humidity increments which have a similar vertical structure but with lower values by about 30% compared to the control experiment (see Fig. 7). Although there is an impact on the results when a high observation error for moderate and heavy rainrate is assumed, 1D-Var is still able to assimilate information from observations as shown by the reduction of the standard deviation and by the non-negligible humidity increments obtained.

A second test on the observation error has been done. It concerns the threshold value imposed for light rainrates. Since the 2A12 algorithm from which mean surface rainrates are obtained performs generally well to identify non-rainy pixels, a smaller threshold error for low mean observed rainrates was set: 0.001 mm h^{-1} instead of 0.01 mm h^{-1} (experiment noted Test 2). Results for $(R_a - R_o)$ bias and standard deviation are nearly identical for Test 2 and Control (see Table 2). Increment profiles of temperature and humidity are also very close except for some profiles where Test 2 provides very large increments in absolute values for temperature (up to 7 K) and specific humidity (up to 3.5 g/kg). For these "pathological" profiles, the weight given to the observation term in the cost-function is obviously too large and therefore almost relaxes the background constraint. Thus, 1D-Var analysis cannot accept a too small observation error.

Experiment	Analysis date/time	$(R_b - R_o)$ in mm h^{-1} Bias / Std	$(R_a - R_o)$ in mm h^{-1} Bias / Std
Control	11 Feb. 1998 00 UTC	0.12 / 2.01	-0.11 / 0.80
Control	26 Aug. 1998 12 UTC	0.22 / 2.18	-0.09 / 1.09
Test 1	11 Feb. 1998 00 UTC	0.12 / 2.01	-0.22 / 1.25
Test 2	11 Feb. 1998 00 UTC	0.12 / 2.01	-0.11 / 0.80
Test 3	11 Feb. 1998 00 UTC	0.13 / 2.02	-0.12 / 0.82
Test 4	11 Feb. 1998 00 UTC	0.21 / 1.96	-0.12 / 1.04
Test 4	26 Aug. 1998 12 UTC	0.43 / 1.78	-0.04 / 0.99

Table 2: *Statistics on 1D-Var results for Control and Test experiments. In Test 1, the observation error for moderate and high rainrates in doubled. In Test 2, the observation error threshold for light rainrates is decreased. In Test 3, the control vector only includes specific humidity profiles. In Test 4, observations are taken at the middle of the 6-hour assimilation window.*

5.3 Reduced control vector

It was shown in section 4 that 1D-Var analysis essentially modifies specific humidity profiles to improve model rainrate while providing very small increments of temperature. Thus, a possibility to decrease the computational cost of 1D-Var is to reduce the control vector by not modifying the temperature profiles. A test (experiment noted Test 3) was done in which temperature profiles are only used as background information in the observation operator. Results given in Table 2 show that the bias and the standard deviation of $(R_a - R_o)$ are both very close to those of the control experiment. The difference between the Control and Test 3 experiment for relative humidity increments (Fig 7c) is rather small showing that the minimization finds a similar solution in terms of atmospheric state. However, mean increments of specific humidity for Test 3, displayed in Figure 7b, are larger by about 50 % in absolute values than the Control experiment for both LESS and MORE profiles. Since in this case the minimization can only act on specific humidity, modifications have to be larger than when temperature is also used in the control vector for producing equivalent rainfall increments. Using only specific humidity profiles and surface pressure as control variables can reduce 1D-Var computational cost but modifies noticeably the analysed specific humidity state.

5.4 Number of time slots

The impact of assimilating the 6-hour data set at the middle time of the assimilation window instead of at the appropriate observation time (7 time slots) is examined (experiment noted Test 4). The mean surface rainrate used for Test 4 has been calculated as described in section 3 but using the whole six-hour data set. In areas that are sampled several times by TMI in six

hours (subtropical regions) the resulting field is the mean of the different overpasses. For fast moving systems, this can lead to a slightly different rainfall field, as illustrated by the front case (Fig. 9) which was sampled at three different times during the 6 hour window: 10 Feb. 1998 around 2305 UTC, 11 Feb. 1998 around 0045 UTC and 11 Feb. 1998 around 0220 UTC. The resulting field is more extensive and less intense than that obtained only using the overpass on 10 Feb. 1998 around 2305 UTC (Fig 1c).

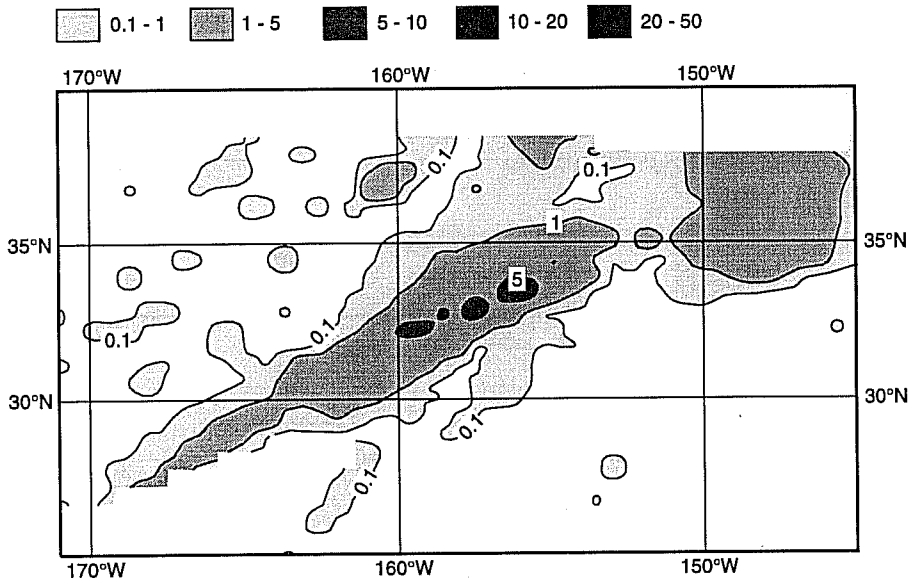

Figure 9: *Same as Figure 1c but for the R_o field used in Test 4 experiment (see text for explanations).*

Test 4 evaluates the hypothesis that precipitation does not vary much in intensity and location within six hours. Although this hypothesis is not always fulfilled as illustrated by Figure 9, the impact on the 1D-Var analysis tends be limited. The rainfall field analysed for Test 4 experiment is displayed in Figure 10. Comparison between R_a fields for Control and Test 4 experiments exhibits small differences which are related to the use of a slightly different background field and of a slightly different observation field for the front case. General results given in Table 1 show that the number of points analysed in Test 4 is reduced by 17 % for the February case and of 15 % for the August case because of a reduced number of observations. The bias $(R_b - R_o)$ is increased mainly because of the use of background field at a single time and also because of the slight decrease of R_o values in subtropical regions. The bias and standard deviation of $(R_a - R_o)$ for Test 4 are close to those found in the Control experiment. Increments for temperature, specific humidity and relative humidity for LESS profiles are the same between Test 4 and the Control experiment (Fig. 7). Test 4 increments for MORE profiles are slightly smaller in absolute value because in this case the R_o field is slightly weaker in regions that are sampled more that once. All these results indicate that the reduction of the number of time slots from seven to one does not change much the 1D-Var results while it allows an easier implementation in 4D-Var. The impact of this configuration should be tested in the 4D-Var assimilation framework.

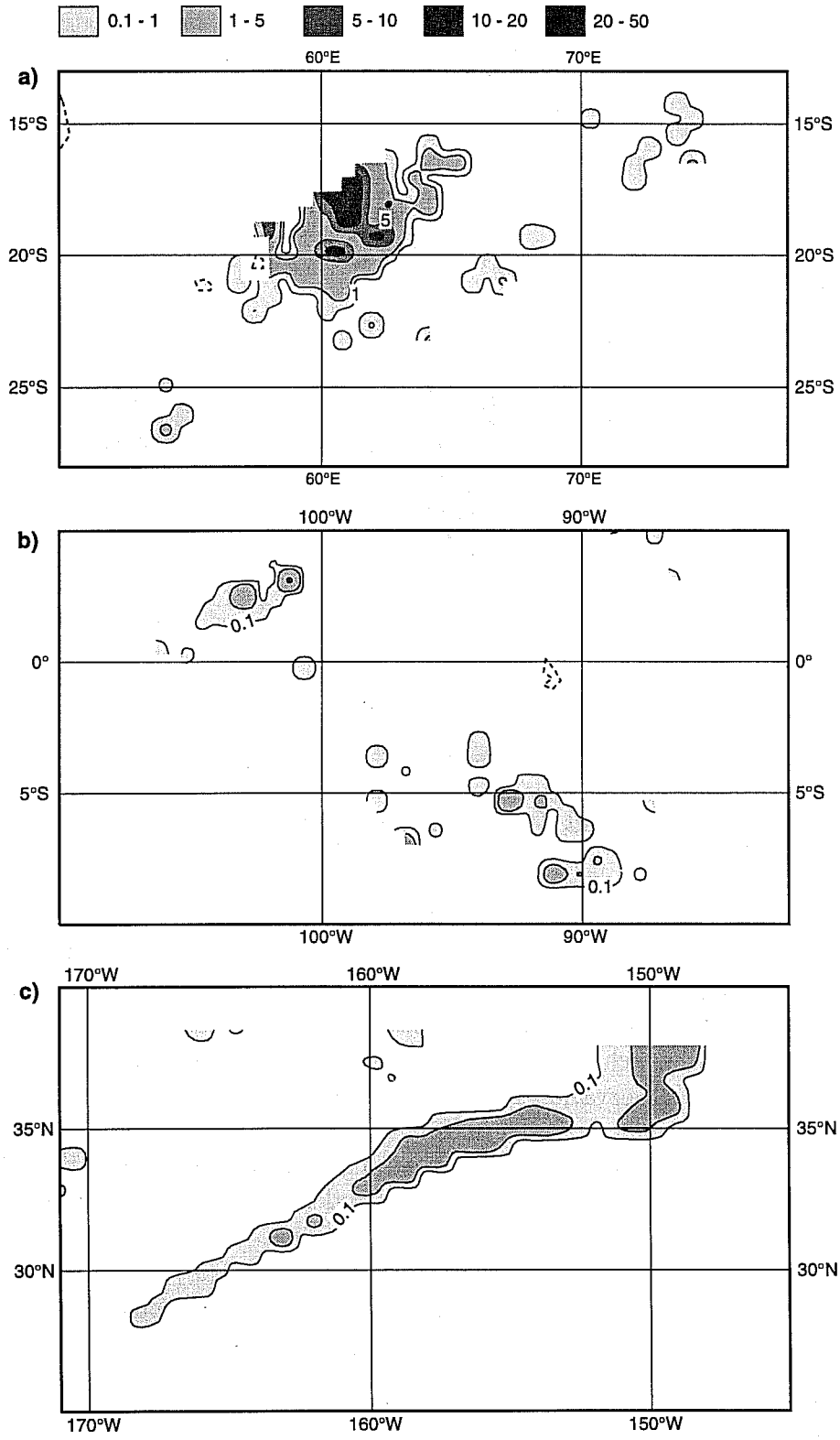

Figure 10: *Same as Figure 1 but for 1D-Var analysed surface rainrate (R_a field) for Test 4 experiment. Background surface rainrate is used for grid points not satisfying the criteria of formula (3).*

6 Conclusions

This paper presents results from a 1D-Var assimilation of TMI derived surface rainrate fields. The 1D-Var method allows to retrieve temperature and humidity profiles that provide precipitation close to observations while remaining consistent with a model short-range forecast.

A 1D-Var scheme has been adapted from Fillion and Mahfouf (1999) [FM99] using the ECMWF mass-flux convection scheme. A diagnostic large-scale condensation scheme (ST) is coupled to the convection scheme in a Fractional-Stepping mode (Beljaars, 1991). A major difference with FM99 version is the use of rainrates observations from TMI radiometer instead of simulated observations. The introduction in the observation operator of the background profiles of temperature and specific humidity time tendencies due to other processes (dynamics, radiation, turbulence and gravity wave drag) has provided information on the thermodynamic environment of the considered profiles. They proved to be essential in order to get consistency between 1D-Var and 4D-Var background precipitation fields (i.e. model short-range forecast). Nevertheless, frontal precipitation is always weaker and less spread in the 1D-Var background field due to the use of a diagnostic ST scheme in 1D-Var which is less efficient than the operational prognostic ST scheme that uses more explicitly the model dynamics.

When the background rainrate field is non-zero, results have shown that 1D-Var assimilation is generally able to increase, decrease, and switch-off precipitation to get closer to observations. For heavy precipitation, analysed rainrates are always lower than observed ones due to the model inability to produce very high rainrates and to the specification of large observation errors. Results also clearly showed that some profiles remain almost unchanged by 1D-Var while a modification of the surface rainrate is expected. These profiles should not be assimilated in 4D-Var and a quality control has been proposed before assimilation of 1D-Var products in 4D-Var. When the background precipitation is zero, 1D-Var is not able to trigger precipitation where it exists in the observations. This is a major weakness of the 1D-Var approach that will need to be addressed in future developments. The 1D-Var analysis provides mean temperature increments less than 0.1 K over the whole atmosphere while mean specific humidity increments are greater than 0.35 g kg^{-1} around model level 25 (about 800 hPa). As a consequence, 1D-Var products related to specific humidity such as total column water vapour can be assimilated in 4D-Var without significant loss of information.

Because no precise information on observation error is yet available to quantify the uncertainty of the precipitation retrievals, sensitivity tests on the mean surface rainrate error values have been done. An increase of the error from $0.25 \times R_o$ to $0.50 \times R_o$ for moderate and heavy rainrates leads to a 30 % decrease of the specific humidity increments and to an increase of the standard deviation for $(R_a - R_o)$. Nevertheless, there is a noticeable improvement of the model precipitation with respect to observations even when a large value is used. A reduction of the threshold observation error value used for light and zero rainrates does not change the results except for few profiles where unrealistic increments of temperature and specific humidity are found. To avoid this problem, a threshold value of at least 0.01 mm h^{-1} should be used.

This 1D-Var retrieval is the first step toward the use of TMI data in the ECMWF 4D-Var system. The second step is the assimilation of 1D-Var products in the ECMWF 4D-Var assimilation system. In order to reduce the computation cost of 1D-Var, two approaches have been tested. The first one uses a reduced control vector by not modifying temperature profiles. In the second test one single background field and one single observation field are used instead of seven for each assimilation window. Although it assumes the steadiness of precipitation over a period of six hours, which is not always true, results are very similar to the Control experiment. Further work needs to be done to evaluate the impact of such possible simplifications on the 4D-Var assimilation of the 1D-Var products.

In the absence of information on observation errors and for simplicity, a Gaussian distribution of the observation error has been assumed in 1D-Var. Errico et al. (1999) showed theoretically that 1D-Var results can depend on the form of the distribution chosen which is likely not Gaussian. New tests of 1D-Var retrieval will be done when a reliable estimation of the distribution form and parameters of the errors will be available from TMI data. In this study, the observation operator was assumed to be error free because no estimation of this error has yet been done. This has to be improved in the future. Indeed, precipitation observations from TRMM represent an ideal data set to assess the accuracy of moist parameterization schemes.

Acknowledgements

TRMM is a joint NASA/NASDA mission (spacecraft launched in November 1997). We acknowledge NASA and NASDA for opening the TRMM data to EuroTRMM, a consortium of scientists from Centre d'étude des Environnements Terrestre et Planétaires (France), German Aerospace Research Establishment (Germany), Istituto di Fisica dell'Atmosfera (Italy), Max Planck Institute für Meteorologie (Germany), Rutherford Appleton Laboratory (U.K.), University of Essex (U.K.), Université Catholique de Louvain (Belgium), University of Munich (Germany) and European Centre for Medium-Range Weather Forecasts (U.K.). EuroTRMM is funded by European Commision and European Space Agency. We thank F. Bouttier for providing us the statistics of forecast errors from the ECMWF operational data assimilation system. Thanks are also due to the INRIA (Institut National de Recherche en Informatique et Automatique) for providing the M1QN3 minimization code used in this study. Tony Hollingsworth, Martin Miller and Luc Fillion provided valuable suggestions for improving the earlier versions of this paper.

References

Beljaars, A.C.M. , 1991: Numerical schemes for parameterizations. *ECMWF Seminar on Numerical methods in atmospheric models*, pages 1-42, ECMWF, Shinfield Park, Reading,

U.K., 9-13 September 1991.

Derber, J. and Bouttier, F. , 1999: A reformulation of the background error covariance in the ECMWF global data assimilation system. *Tellus*, **51A**, 195–221.

Errico, R.M. and Rasch, P.J. , 1988: A comparison of various normal-mode initialization schemes and the inclusion of diabatic processes. *Tellus*, **40A**, 1–25.

Errico, R.M., Fillion, L., Nychka, D. and Lu, Z.-Q. , 1999: Some statistical considerations associated with the data assimilation of precipitation observations. *Quart. J. Roy. Meteor. Soc.*, (accepted for publication)

Fillion, L. and Errico, R. , 1997: Variational assimilation of precipitation data using moist convective parameterization schemes: a 1D-Var study. *Mon. Weather Rev.*, **125**, 2917–2942.

Fillion, L. and Mahfouf, J.-F. , 1999: On the coupling of moist-convective and stratiform precipitation processes for variational data assimilation. *Mon. Weather Rev.*, (accepted for publication)

Gilbert, J.-C., and Lemaréchal, C. , 1989: Some numerical experiments with variable-storage quasi-Newton algorithms. *Math. Programming*, **45**, 407–435.

Gregory, D., Morcrette, J.-J., Jakob, C., Beljaars, A.C.M. and Stockdale, T. , 1999: Revision of convection, radiation and cloud schemes in the ECMWF Integrated Forecasting System. *Quart. J. Roy. Meteor. Soc.* (submitted)

Heckley, W.A., Kelly, G. and Tiedtke, M. , 1990: On the use of satellite-derived heating rates for data assimilation within the tropics. *Mon. Weather Rev.*, **118**, 1743–1757.

Houze, R.A. , 1997: Stratiform precipitation in regions of convection : A meteorological paradox? *Bull. Amer. Meteor. Soc.*, **78**, 2179–2196.

Krishnamurti, T.N., Ingles, K., Cooke, S., Kitade, T. and Pasch, R. , 1984: Details of low-latitude, medium-range numerical weather prediction using a global spectral model. Part 2 : Effects of orography and physical initialization. *J. Meteor. Soc. Japan*, **62**, 613–648.

Krishnamurti, T.N., Bedi, H.S. and Ingles, K. , 1993: Physical initialization using SSM/I rain rates. *Tellus*, **45A**, 247–269.

Kummerow, C., Olson, W. and Giglio, L. , 1996: A simplified scheme for obtaining precipitation and vertical hydrometer profiles from passive microwave sensors. *I.E.E.E. Trans. Geosci. Remote Sensing*, **34**, 1213–1232.

Kummerow, C., Barnes, W., Kozu, T., Shiue, J. and Simpson, J. , 1998: The Tropical Rainfall Measuring Mission (TRMM) Sensor Package. *J. Atmos. Ocean. Technol.*, **15**, 809–817.

Parrish, D.F. and Derber, J.C. , 1992: The National Meteorological Center's Spectral Statistical Interpolation Analysis System. *Mon. Weather Rev.*, **120**, 1747–1763.

Puri, K. and Miller, M.J. , 1990: The use of satellite data in the specification of convective heating for diabatic initialization and moisture adjustment in numerical weather prediction models. *Mon. Weather Rev.*, **118**, 67–93.

Rabier, F., McNally, A., Andersson, E., Courtier, P., Unden, P, Eyre, J., Hollingsworth, A. and Bouttier, F. , 1997: The ECMWF implementation of three dimensional variational assimilation (3D-Var). Part II: Structure functions. *Quart. J. Roy. Meteor. Soc.*, **124**, 1809–1829.

Rabier, F., Järvinen, H., Klinker, E., Mahfouf, J.-F. and Simmons, A. , 1999: The ECMWF operational implementation of four dimensional variational assimilation. Part I: Experimental results with simplified physics. *Quart. J. Roy. Meteor. Soc.* (accepted for publication)

Simpson, J., Kummerow, C., Tao, W.-K., and Adler, R.F., 1996: On the Tropical Rainfall Measuring Mission (TRMM). *Meteor. Atmos. Phys.*, **60**, 19–36.

Tiedtke, M., 1989: A comprehensive mass flux scheme for cumulus parameterization in large-scale models. *Mon. Weather Rev.*, **117**, 1779–1800.

Tiedtke, M., 1993: Representation of clouds in large-scale models. *Mon. Weather Rev.*, **121**, 3040–3061.

Treadon, R.E. , 1996: Physical initialization in the NMC global assimilation system. *Meteorol. Atmos. Phys.*, **60**, 57–86.

Treadon, R.E. , 1997: Assimilation of satellite derived precipitation estimates with the NCEP GDAS. *Ph.D. Dissertation, Florida State University*, 348 pp.

Tsuyuki, T. , 1996a: Variational data assimilation in the Tropics using precipitation data. Part I: Column model. *Meteor. Atmos. Phys.*, **60**, 87–104.

Tsuyuki, T. , 1996b: Variational data assimilation in the Tropics using precipitation data. Part II: 3D-model. *Mon. Weather Rev.*, **124**, 2545–2561.

Tsuyuki, T. , 1997: Variational data assimilation in the Tropics using precipitation data. Part III: Assimilation of SSM/I precipitation rates. *Mon. Weather Rev.*, **125**, 1447–1464.